



Available online at
ScienceDirect
 www.sciencedirect.com

Elsevier Masson France
EM|consulte
 www.em-consulte.com



Original Article

Smelling decides: fMRI evidence reveals the influence of olfactory stimuli on risky decision-making

Amir Hossein Dakhili^{a,c}, Seyed Kamran Kamrava^b, Arash Zare-Sadeghi^{c,*}

^a Neuroscience of Addiction and Mental Health Program, Healthy Brain and Mind Research Centre, School of Behavioral and Health Sciences, Faculty of Health, Australian Catholic University, Fitzroy, Victoria, Australia

^b ENT Research Center, Institute of Five Senses, Hazrat Rasoul Hospital, Iran University of Medical Sciences, Tehran, Iran

^c Finetech in Medicine Research Center, Medical Physics Department, School of Medicine, Iran University of Medical Sciences, Tehran, Iran

ARTICLE INFO

Keywords:

Risky decision-making
 fMRI
 Functional connectivity
 Olfactory stimuli
 Gambling

ABSTRACT

Background and purpose: Olfactory stimuli are known to have a significant effect on cognitive functions. However, their effect on risky decision-making remains unclear. The present study aimed to investigate this effect, using functional magnetic resonance imaging (fMRI) and a novel mixed gambling task.

Materials and Methods: Twenty-nine healthy participants with normal olfactory function underwent fMRI scanning while performing a gambling task under exposure to pleasant and unpleasant odors, as well as fresh air and a neutral condition without any olfactory stimulation. ROI-to-ROI functional connectivity analyses were conducted, focusing on regions involved in olfactory processing and risky decision-making, including dorsolateral prefrontal cortex (DLPFC), ventromedial prefrontal cortex (vmPFC), orbitofrontal cortex (OFC), insula, anterior cingulate cortex (ACC), piriform cortex, and uncus.

Results: Pleasant odors, compared to the neutral condition, enhanced connectivity between OFC and vmPFC. Fresh air, compared to neutral, reduced connectivity between the DLPFC, OFC, vmPFC, piriform and insula, while increasing connectivity between the piriform and uncus. Unpleasant odors, compared to neutral, increased connectivity between the vmPFC, OFC, and ACC. Unpleasant odors, compared to fresh air, enhanced connectivity between the DLPFC and insula but reduced connectivity between the insula and OFC. Pleasant odors, compared to unpleasant odors, increased connectivity between the insula and OFC (p -FDR < 0.05).

Conclusion: Olfactory stimuli modulate neural networks underlying risky decision-making during a mixed gambling task. These findings highlight the clinical relevance of olfactory modulation for addiction research and the potential of functional connectivity analyses to provide a foundation for personalised interventions aimed at reducing maladaptive risk-taking behavior and cue-driven vulnerability.

Introduction

Decision-making is a complex cognitive function influenced by factors such as individual traits, demographic characteristics, beliefs, and past experiences.^{1–4} Among the various aspects of decision-making, those associated with risks (i.e., risky decision-making) are a common part of our daily interactions. Risky decision-making refers to choices made between alternatives with uncertain outcomes that depend on changing circumstances and their probabilities.⁵

While the influence of social and cultural factors on risky decision-making has been widely studied, the role of intrinsic sensory factors and their effect on neural correlates of risky decision-making remains less understood. One such overlooked factor is olfaction. Olfaction has been shown to strongly influence a wide range of cognitive processes.^{6–14}

Evidence indicates that certain odors enhance cognitive functions, including memory, attention, pain perception, self-perception, and alertness.^{10–19} Yet, the influence of olfactory stimuli on risky decision-making remains underexplored.^{20–22}

Current literature has provided partial insights into how odors influence decision-making. For instance, exposure to mint aroma has been shown to reduce risk-taking behaviors²³, whereas a gambling study found that participants exposed to pleasant odors were more likely to engage in gambling behavior.²⁴ Neuroimaging findings show that olfactory information is initially processed in primary olfactory regions, including the piriform cortex and uncus, which play a key role in encoding odor identity and affective significance and maintain strong anatomical and functional connections with limbic and prefrontal regions.^{25–28}

*Corresponding author at: Finetech in Medicine Research Center, Medical Physics Department, School of Medicine, Iran University of Medical Sciences, Shahid Hemmat Highway, Tehran 1449614535, Iran.

E-mail address: zare.a@iums.ac.ir (A. Zare-Sadeghi).

<https://doi.org/10.1016/j.neurad.2026.101529>

Available online 5 February 2026

0150-9861/© 2026 Published by Elsevier Masson SAS.

Beyond primary olfactory processing, the left orbitofrontal cortex (OFC) has been consistently implicated in value-based decision-making during exposure to olfactory stimuli.²⁹ Additionally, olfactory stimulation can increase activation in the anterior cingulate cortex (ACC) and dorsolateral prefrontal cortex (DLPFC) during decision-making tasks.³⁰ Another study found that unpleasant odors were associated with increased activation in the ventromedial prefrontal cortex (vmPFC) during moral decision-making tasks.³¹ Further studies revealed an increase in the activation of DLPFC, and insula when participants were assessing the intensity and pleasantness of olfactory stimuli.³² However, these studies primarily examined localised activation patterns and offer limited understanding of how olfactory stimuli alter the functional interactions between brain regions involved in olfactory processing and risky decision-making.

Functional magnetic resonance imaging (fMRI) is a widely used technique to study the neural processes involved in decision-making.³³ While traditional task-based fMRI analyses identify region-specific activations, they do not fully capture the dynamic connectivity between regions that supports complex cognitive processes. Functional connectivity analyses, provide a means to assess coordinated activity across distributed neural networks during cognitive processes, including risky decision-making.³⁴ Importantly, the sensitivity of task-based fMRI to such network dynamics depends not only on the analytical approach but also on the behavioral paradigm employed. While some tasks like the Monetary Incentive Delay (MID) task are widely used for isolating the neural correlates of reward anticipation and outcome processing, they primarily engage incentive-motivational circuitry rather than the active evaluative processes required for risky decision-making.^{35, 36} In contrast, gambling paradigms directly engage decision-making under uncertainty by requiring explicit evaluation of potential gains and losses at the moment of choice, and recruiting neural systems involved in risk appraisal and value comparison.^{37–39}

We sought to address the current gaps by developing a novel fMRI paradigm that integrates a gambling task with olfactory stimulation to investigate how different olfactory stimuli (pleasant, unpleasant, and fresh air) modulate patterns of functional connectivity within brain regions involved in olfactory processing and risky decision-making.

Method and material

Participants

Thirty-four healthy individuals aged 18–40 were initially screened for participation in this study. Eligibility was determined by two primary criteria: (1) a minimum of twelve years of formal education and (2) normal olfactory function. Exclusion criteria were defined as follows: (1) broncho-pulmonary or neurological conditions, (2) chronic pain, (3) pregnancy or breastfeeding status, (4) current cold or allergy symptoms, (5) an allergy to perfumes, (6) current use of analgesic medication including non-prescription drugs, (7) failure in an olfactory assessment, (8) MRI incompatibilities such as metal implants or claustrophobia, (9) a history of head trauma leading to neurological consequences, or (10) any neurological disorder that might influence the outcome of the study. Participants were also instructed to avoid wearing scented products on the day of testing. All procedures adhered to the Declaration of Helsinki guidelines, with data anonymised prior to analysis. Ethical approval was obtained from the Iran University of Medical Sciences, under the code IR.IUMS.FMD.REC.1400.101.

Measures and questionnaires

Potential participants underwent a medical evaluation by a physician. Demographic data were collected prior to any scanning procedures. Before the imaging session, participants familiarised themselves with the gambling task at the Iran University of Medical Sciences laboratory, emphasising both speed and accuracy of task performance.

Olfactory function was assessed using the Sniffin Sticks test kit (Burghart Instruments, Wedemark, Germany). This kit comprises three subtests, measuring odor threshold, odor discrimination, and odor identification. Odors were presented using pen-like instruments, following standardised protocols.^{40–42} For determining odor detection thresholds, a single-staircase, three-alternative forced-choice procedure was employed. The odor discrimination subtest consisted of 16 trials, each presenting participants with three different odorants. Within each set, two odorants were identical, and one was different. Participants were asked to identify the distinct odorant. In the odor identification subtest, participants were exposed to 16 common odors and asked to select the correct descriptor from four possible options. Scoring was based on established guidelines: the odor detection threshold ranged from 1 to 16 points, while the discrimination and identification subtests each ranged from 0 to 16 points. The sum of all three subtests produced the Threshold–Discrimination–Identification (TDI) score. A TDI score of 30.5 or above indicated normosmia; scores between 16.5 and 30 suggested hyposmia; and scores below 16 were indicative of functional anosmia.⁴³

fMRI gambling task

Fig. 1 shows the experimental design of the fMRI task and the study protocol. Participants underwent two consecutive fMRI runs implementing a block-design gambling task, followed by resting blocks displaying a fixation cross. Within each run, four 60-second blocks were presented, and in each block, participants performed four gambling trials. In each trial, participants were presented with four selectable values ($A = 0$, $B = 5$, $C = 15$, $D = 25$) and were asked to combine these values in any way they preferred, such as choosing multiple instances of the same value or mixing different ones, to calculate a total sum within 13 s using a button box. Each trial was followed by a jittered interstimulus interval (ISI), which averaged 1 s. When the calculated sum was within 10 units of a computer-generated target, the feedback “You won!” appeared; otherwise, “You lost!” was displayed. The task consisted of four experimental conditions: The first, neutral condition, exposed participants to the ambient air in the scanner without added scents or airflow modulation. The second, pleasant odor condition, introduced a vanilla scent (vanilla diluted in a solution of ethanol and water (200gr per liter)), through an olfactometer described in the section below. The third, fresh air condition, delivered an increased flow of unscented air, distinguishing it from the neutral state. The final, unpleasant odor condition, presented the odor of phenol glycerin (6.4 % phenol in glycerin base, $C_6H_{12}O_3$). Each task block was separated by an 87-second rest period indicated by a white cross on a black background. Each run lasted 9 min and 48 s.

Olfactometer setup

Olfactory stimuli were delivered using a custom-built olfactometer comprising an air supply, control unit, and airflow distribution system (Fig. 1). Filtered and odorless air (30 L/min) was regulated and divided into eight channels, each connected to an odor reservoir via solenoid valves. During stimulation, the air stream (4 L/min) passed through the selected odor chamber (vanilla or phenol glycerin) and was conveyed via a 4-meter silicone tube (inner diameter = 4 mm [mm]) to a nasal mask fitted on the participant’s face in the scanner. The olfactometer was deactivated during the neutral condition.

Scanning parameters

Scanning was conducted in a 3.0 Tesla (Siemens, MAGNETOM Prisma; Germany) MR-system at the National Brain Mapping Laboratory, Tehran, Iran. Structural T1-weighted images were acquired in a sagittal orientation employing a magnetisation-prepared rapid gradient-echo (MP-RAGE) sequence with the following parameters: Repetition Time = 1830 milliseconds (ms), Echo Time = 3.5 ms, field of view (FOV) = 256 cm × 256 cm, flip angle (FA) = 7°, 1 mm³ voxels. A

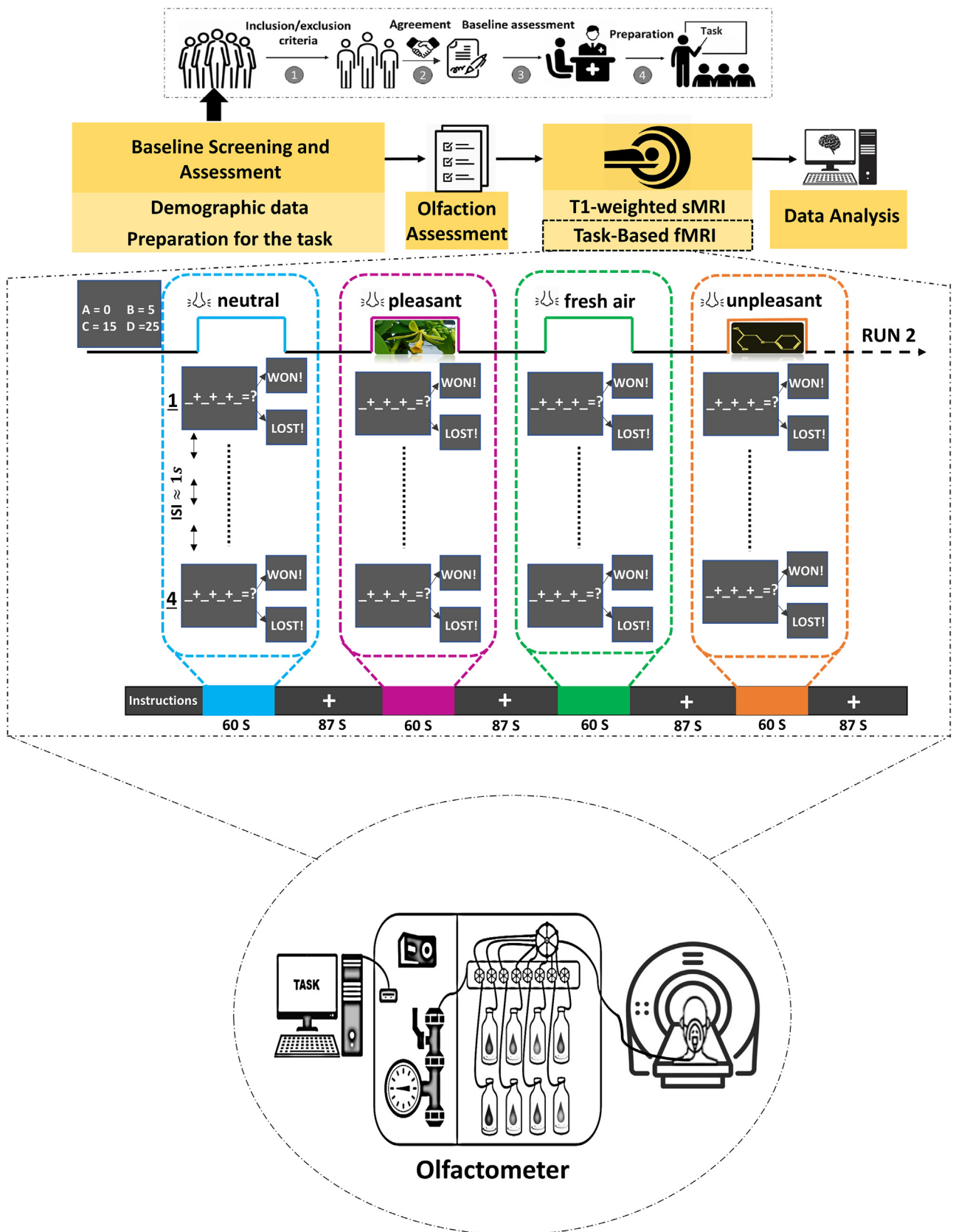


Fig. 1. Task design and study protocol.

gradient-echo-planar imaging (GRE-EPI) sequence with the following parameters was used to obtain functional MRI data: TR = 2000 ms, TE = 30 ms, FOV = 192 192, FA = 80, and in-plane voxel size of 2 mm.

fMRI data analysis

Initial preprocessing of functional images was performed using the fMRI Expert Analysis Tool (FEAT), a component of the FMRIB Software Library (version 6.0.3), while subsequent denoising and all functional connectivity analyses were conducted in the CONN toolbox. The preprocessing procedure, using FEAT, consisted of the following steps: (1) skull-stripping to remove nonbrain tissue from structural T1-weighted images using the Brain Extraction Tool (BET) with default values; (2) interleaved slice-timing correction; (3) motion correction with 6 degrees of freedom (DOF); (4) registration of the functional images to individual structural images using FMRIB's Linear Image Registration (FLIRT) and Boundary Registration (BBR) cost function; (5) normalization of structural images to MNI standard space; (6) spatial smoothing with a Gaussian kernel with a full-width at half maximum (FWHM) of 4 mm; (7) multiplicative normalization of the volume's mean intensity at each time point; (8) high-pass temporal filtering (Gaussian weighted least-squares straight-line fitting, with an Inverse of = 120.0 s). Analyses of functional connectivity were conducted with the CONN toolbox (version 20.b, www.nitrc.org/projects/conn, RRID:SCR 009,550)⁴⁴ in Statistical Parametric Mapping toolbox (SPM8, Wellcome Centre for Human Neuroimaging, University College London, UK; www.fil.ion.ucl.ac.uk/spm). In accordance with the standard scrubbing procedures for the removal of confounders in the CONN toolbox, the nuisance regression included motion parameters, linear detrending, and aCompCor components derived from white matter and cerebrospinal fluid signals.⁴⁵ Time series were temporally filtered using a band-pass filter of 0.008–0.09 Hz.⁴⁶

Regions of interest (ROIs) were defined based on their established involvement in olfactory processing and decision-making networks and included the dorsolateral prefrontal cortex (DLPFC), orbitofrontal cortex (OFC), anterior cingulate cortex (ACC), insula, ventromedial prefrontal cortex (vmPFC), piriform cortex, and uncus. The DLPFC mask was extracted using the Brainnetome Atlas⁴⁷, specifically targeting subregions A9l (lateral Area 9) and A46 (Area 46) in line with previous studies.^{48–51} Anatomical masks of OFC, insula, and ACC were defined bilaterally using the Automated Anatomical Labeling (AAL) atlases⁵², and extracted using the WFU PickAtlas toolbox (<http://fmri.wfubmc.edu/software/PickAtlas>) in MATLAB 2021a (<https://www.mathworks.com/products/matlab.html>) and FSLeys (<https://fsl.fmrib.ox.ac.uk/fsl/fslwiki/FSLeys>). The bilateral mask of vmPFC was created by combining bilateral orbital frontal regions and rectus regions from the AAL atlas.^{53, 54} The bilateral mask of piriform cortex was defined as 10 mm radius spheres centered at MNI coordinates [–22, 0, 14] and [22, 2, 12], which have been previously reported to show activation during olfactory stimulation.^{55–57} The bilateral mask of uncus was defined as 10 mm radius spheres centered at MNI coordinates [14, –12, –22] and [–16, –12, –24].⁵⁸

Condition-specific regressors (neutral, pleasant odor, fresh air, unpleasant odor) were modeled using their respective onsets and durations and convolved with a canonical hemodynamic response function. ROI-to-ROI functional connectivity was computed using Fisher z-transformed correlation coefficients between ROI time series for each condition.

At the second level, ROI-to-ROI connectivity analyses were performed using general linear models (GLMs) implemented in the CONN toolbox. To account for potential gender-related effects on functional connectivity, gender was included as a covariate of no interest in all second-level analyses. Connectivity differences between conditions were assessed using contrast-based *t*-tests, with statistical significance determined using false discovery rate (FDR) correction across ROI-to-ROI connections at *p*-FDR < 0.05.

Results

Participants characteristics

Out of the initial thirty-four participants, four participants did not meet the inclusion criteria, and data from one additional participant were excluded due to excessive motion during scanning. Consequently, data from 29 participants (16 females; mean age = 24.76 years) were included in the final fMRI analysis (Table 1).

Olfaction assessment

Results of the Sniffin' Sticks test indicated normal olfactory function across all participants, with comparable performance between males and females (Table 1).

ROI-to-ROI functional connectivity

pleasant odor > neutral

In the pleasant odor > neutral contrast, increased connectivity was observed between the OFC as the seed region and vmPFC (*t*-value = 3.30, *p*-FDR = 0.0165) (Fig. 2, Table 2).

fresh air > neutral

This contrast revealed increased connectivity between piriform and uncus (*t*-value = 2.93, *p*-FDR = 0.0204), OFC and vmPFC (*t*-value = 3.47, *p*-FDR = 0.0053), and between vmPFC and insula (*t*-value = 2.57, *p*-FDR = 0.0321). In addition, decreased connectivity was observed between DLPFC as seed region and OFC (*t*-value = –3.73, *p*-FDR = 0.0053), piriform (*t*-value = –3.10, *p*-FDR = 0.0136), vmPFC (*t*-value = –2.89, *p*-FDR = 0.0151), and insula (*t*-value = –2.25, *p*-FDR = 0.0495) (Fig. 3, Table 2).

unpleasant odor > neutral

This contrast showed an increased connectivity between vmPFC as seed region and ACC (*t*-value = 2.80, *p*-FDR = 0.0284), and OFC (*t*-value = 2.79, *p*-FDR = 0.0284) (Fig. 4, Table 2).

unpleasant odor > fresh air

This contrast revealed increased functional connectivity between DLPFC and insula (*t*-value = –3.89, *p*-FDR = 0.0035) and decreased connectivity between insula and OFC (*t*-value = –2.96, *p*-FDR = 0.0190) (Fig. 5, Table 2).

pleasant odor > unpleasant odor

This contrast showed increased connectivity between insula and OFC (*t*-value = 3.04, *p*-FDR = 0.0309) (Fig. 6, Table 2).

Discussion

This study investigated how different olfactory stimuli modulate neural connectivity underlying risky decision-making, using a novel mixed

Table 1
Demographic characteristics and olfactory performance of participants (*n* = 29).

Variables	Male (<i>n</i> = 13)	Female (<i>n</i> = 16)
Age (years)	25.15 (3.31)	23.81 (3.56)
Education (years)	17.38 (1.60)	17 (2.12)
Smelling Threshold	9.41 (2.39)	9.27 (2.05)
Smelling Detection	13.47 (1.51)	13.35 (1.64)
Smelling Identification	13.91 (1.91)	13.83 (1.43)
TDI	36.79 (1.51)	36.45 (1.71)

Note: values are denoted as mean (SD).

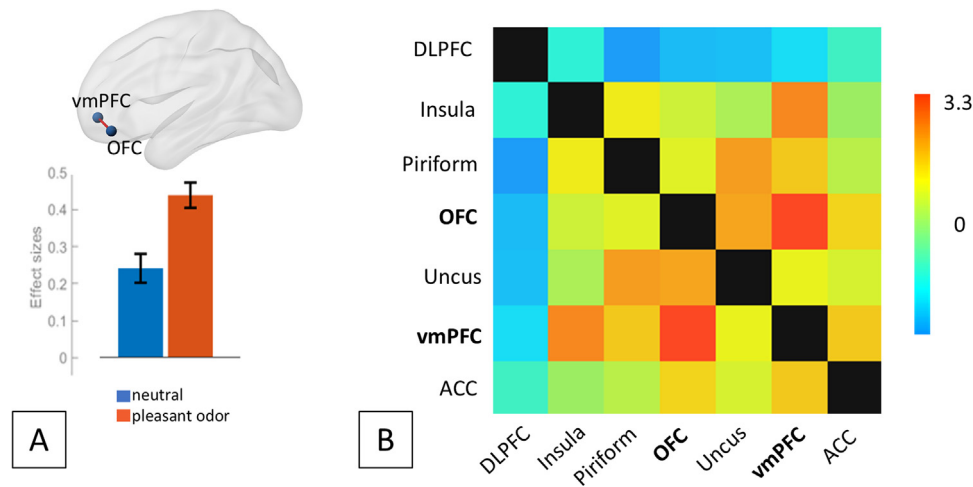


Fig. 2. pleasant odor > neutral contrast.

(A) Effect-size plot showing Fisher z-transformed ROI-to-ROI connectivity across conditions (p-FDR < 0.05). Error bars indicate standard error of the mean.

(B) ROI-to-ROI correlation matrix showing correlation coefficients for each of the 7 × 7 ROI correlations in pleasant odor > neutral contrast. Significant increased connectivity was observed between OFC and vmPFC (p-FDR < 0.05). Colors indicate the magnitude of the T statistic.

fMRI gambling paradigm in healthy participants with normal olfactory function.

pleasant odor > neutral

Results of this contrast revealed enhanced connectivity between the OFC and vmPFC. The increased interaction between the OFC and vmPFC observed here reflects the integration of affective value and sensory information, consistent with evidence that both regions contribute to the evaluation of odor pleasantness.^{58–60}; This pattern of connectivity further supports the validity of the task in engaging affective aspects of olfactory processing. vmPFC is also involved in value-based and risky decision-making processes^{61–65}, suggesting that its engagement here may also show its involvement in reward valuation and outcome anticipation. In parallel, OFC plays a key role in evaluating stimulus value (e.g., reward) and learning stimulus-outcome associations, and disruption in its function have been linked to the risky decision-making and challenges in outcome anticipation.^{66–79} Enhanced connectivity between these regions suggests stronger

integration of affective and evaluative processes when participants were exposed to pleasant odor.

fresh air > neutral

This contrast revealed a pattern of decrease in connectivity between the DLPFC and OFC, piriform, vmPFC, and insula. Previous research indicated that activation of DLPFC associates with decision-making abilities.^{80–83} Reduced functional connectivity between the DLPFC and other cortical regions observed under the fresh air condition may indicate a more optimized engagement of prefrontal control networks during the risky decision-making process.⁸⁴

In contrast, increased connectivity was observed between the OFC and vmPFC, between the vmPFC and insula, and between piriform and uncus. Increased connectivity between the vmPFC and insula underscores the role of the insula in relaying sensory information, including olfactory inputs, from somatosensory regions to the vmPFC.⁸⁵ The insula is also recognised for its involvement in diverse decision-making functions, including attention, value evaluation, choice determination, and reward processing.^{86–91} Moreover, prior studies have highlighted the role of the insula in activating representations of homeostatic states related to the perception of risk, which subsequently impacts decision-making processes.⁹²

The piriform cortex, a key region of the olfactory network, processes information derived from olfactory stimuli and is associated with tasks like odor categorisation and identification.⁹³ Uncus covers the anterior part of the parahippocampal gyrus known as the entorhinal cortex⁹⁴, which is part of the primary olfactory cortex. The observed connectivity between the piriform and uncus, supports prior evidence that the piriform cortex receives top-down modulatory input from the entorhinal cortex, reflecting their role in integrating olfactory information.⁹⁵

unpleasant odor > neutral

Results of this contrast revealed increased connectivity between the vmPFC, taken as the seed region, and both the right OFC and right ACC. As discussed earlier, the increased connectivity between vmPFC and OFC, serves as a marker of odor recognition. Notably, there was an increased connectivity between the right ACC and vmPFC. Previous studies suggest that activation of ACC correlates with proficient decision-making, effective action-outcome learning, and efficient reward processing.^{32,96–102} Activation of ACC has also been shown to increase in relation to the difficulty of decision-making, potentially induced by

Table 2

Results of ROI-to-ROI connectivity analyses across participants (n = 29).

Contrast	Seed region	Target region	t-value	p-FDR
pleasant > neutral	OFC	vmPFC	3.30	0.0165
fresh air > neutral	DLPFC	OFC	-3.73	0.0053
		Piriform	-3.10	0.0136
		vmPFC	-2.89	0.0151
		Insula	-2.25	0.0495
	Piriform	Uncus	2.93	0.0204
	OFC	vmPFC	3.47	0.0053
	vmPFC	Insula	2.57	0.0321
unpleasant > neutral	vmPFC	ACC	2.80	0.0284
		OFC	2.79	0.0284
unpleasant > fresh air	DLPFC	Insula	3.89	0.0035
	Insula	OFC	-2.96	0.0190
pleasant > unpleasant	Insula	OFC	3.04	0.0309

Notes: The table lists significant ROI-to-ROI connectivity effects (p-FDR < 0.05). The p-FDR column indicates FDR-corrected p-values across connections. The t-value column reports the second-level t-statistic associated with each connectivity effect. Seed and target regions refer to the predefined regions of interest included in the ROI-to-ROI analysis. Contrasts indicate the experimental condition comparisons.

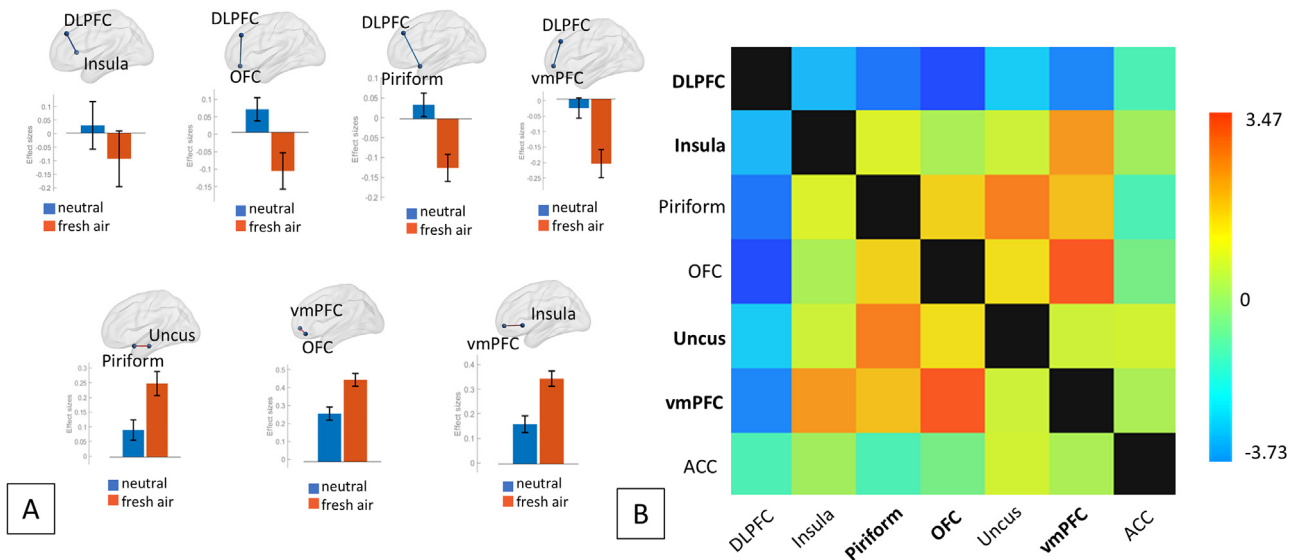


Fig. 3. fresh air > neutral contrast.

(A) Effect-size plot showing Fisher z-transformed ROI-to-ROI connectivity across conditions (p-FDR < 0.05). Error bars indicate standard error of the mean.

(B) ROI-to-ROI correlation matrix showing correlation coefficients for each of the 7 × 7 ROI correlations in fresh air > neutral contrast. Significant increased connectivity was observed between piriform and uncus, OFC and vmPFC, and between vmPFC and insula (p-FDR < 0.05). Significant decreased connectivity was observed between DLPFC and OFC, piriform, vmPFC, and insula (p-FDR < 0.05). Colors indicate the magnitude of the T statistic.

unpleasant odors.¹⁰³ The observed increase in functional connectivity may reflect heightened cognitive demand or decision-making difficulty, consistent with prior evidence that stronger functional connectivity might occur under greater task complexity.^{104,105}

unpleasant odor > fresh air

This contrast showed enhanced connectivity between the DLPFC and the left insula, but decreased connectivity between the insula and left OFC. As previously discussed, both the DLPFC and insula are recognised as key regions for decision-making.^{83,106–108} In addition, some previous research suggests a notable positive correlation between the activation of DLPFC and the complexity of decision-making.^{80–82} The insula has also been shown to increase its activity with greater difficulty of decision-making.¹⁰⁹ Given this, the increased connectivity between the

insula and DLPFC when exposed to unpleasant odors, compared to fresh air, suggests an increased challenge in risky decision-making. In contrast, reduced connectivity between the insula and left OFC might reflect the impaired integration between value perception, risk assessment and outcome prediction.^{110,111}

pleasant odor > unpleasant odor

This contrast revealed enhanced connectivity between the insula and right OFC. Previous literature has shown that both insula and OFC are more activated during risky decision-making.^{112–116} As discussed earlier, the OFC is involved in value perception, and its increased connectivity with the insula, which is involved in risk assessment, may reflect a more integrated evaluation of reward value and potential risk, which facilitates risky decision-making.^{68,69,83,117}

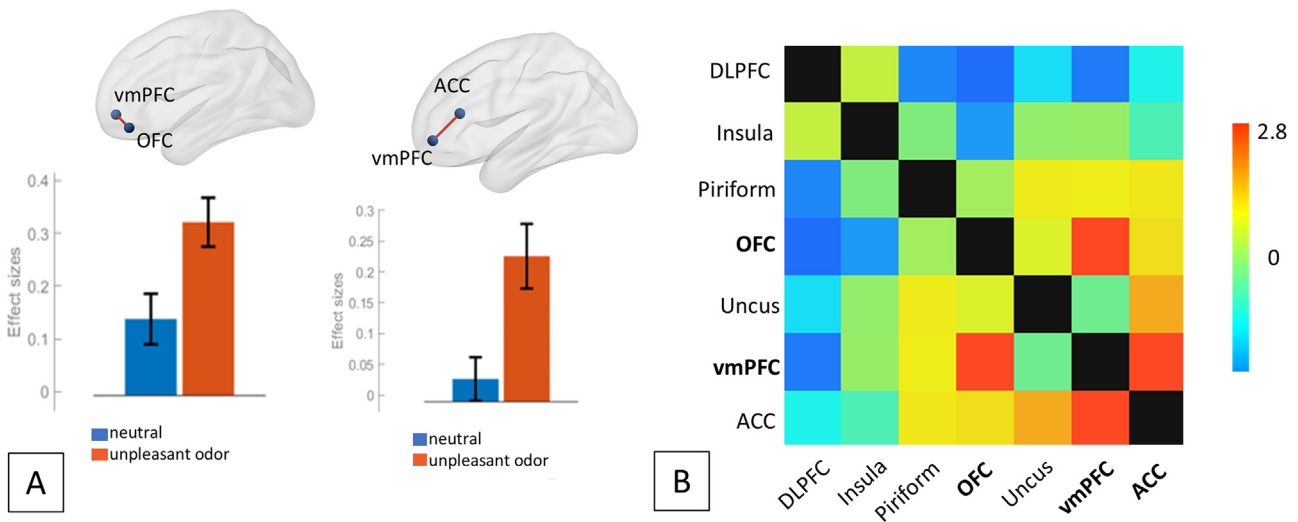


Fig. 4. unpleasant odor > neutral contrast.

(A) Effect-size plot showing Fisher z-transformed ROI-to-ROI connectivity across conditions (p-FDR < 0.05). Error bars indicate standard error of the mean.

(B) ROI-to-ROI correlation matrix showing correlation coefficients for each of the 7 × 7 ROI correlations in unpleasant odor > neutral contrast. Significant increased connectivity was observed between vmPFC and ACC, and between vmPFC and OFC (p-FDR < 0.05). Colors indicate the magnitude of the T statistic.

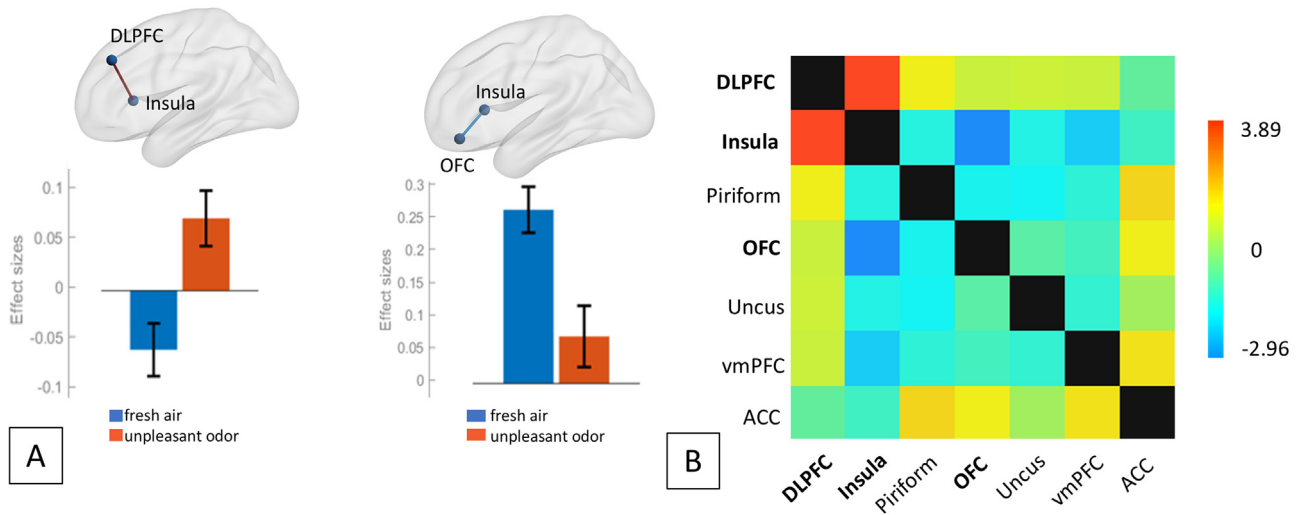


Fig. 5. unpleasant odor > fresh air contrast.

(A) Effect-size plot showing Fisher z–transformed ROI-to-ROI connectivity across conditions (p-FDR < 0.05). Error bars indicate standard error of the mean.

(B) ROI-to-ROI correlation matrix showing correlation coefficients for each of the 7 × 7 ROI correlations in unpleasant odor > fresh air contrast. Significant increased connectivity was observed between DLPFC and Insula (p-FDR < 0.05). Significant decreased connectivity was observed between Insula and OFC (p-FDR < 0.05). Colors indicate the magnitude of the T statistic.

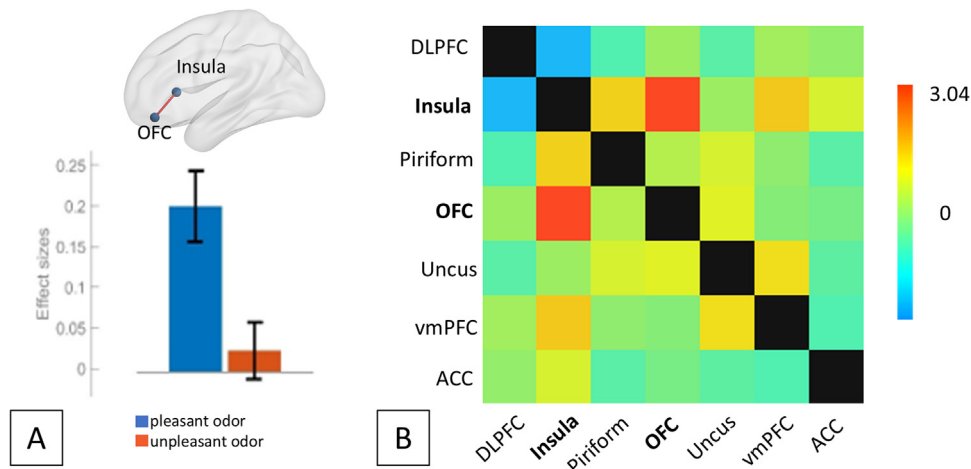


Fig. 6. pleasant odor > unpleasant odor contrast.

(A) Effect-size plot showing Fisher z–transformed ROI-to-ROI connectivity across conditions (p-FDR < 0.05). Error bars indicate standard error of the mean.

(B) ROI-to-ROI correlation matrix showing correlation coefficients for each of the 7 × 7 ROI correlations in pleasant odor > unpleasant odor contrast. Significant increased connectivity was observed between Insula and OFC (p-FDR < 0.05). Colors indicate the magnitude of the T statistic.

Conclusion

This is the first fMRI study to investigate how olfactory stimuli influence neural networks underlying risky decision-making, using a novel mixed gambling task. The findings demonstrate the sensitivity of decision-related networks to sensory environmental cues and highlight the clinical relevance of olfactory modulation for addiction research, including gambling disorder. Moreover, this study highlights the potential of functional connectivity analyses to characterise how sensory cues bias neural networks of risky decision-making and provides a foundation for future research into targeted, personalised interventions aimed at reducing maladaptive risk-taking behavior and cue-driven vulnerability in addiction.

Limitations

This study has several limitations that should be considered when interpreting the findings. First, real-time subjective ratings of odor

perception (e.g., intensity, valence, and arousal) were not collected during scanning. As a result, individual differences in perceptual experience could not be directly assessed during task performance. Future studies would benefit from incorporating subjective odor ratings using Likert or visual analogue scales to provide behavioral context and validate perceptual effects alongside functional connectivity measures. Second, the present analyses focused on connectivity between predefined ROIs and did not examine subregional interactions, which may reveal additional specificity within olfactory and decision-making networks. Finally, future research should explore a wider range of pleasant and unpleasant odors, vary odor intensity levels, and include behavioral measures such as reaction time to better characterise how olfactory stimuli influence risky decision-making.

Role of funding source

Iran University of Medical Sciences approved and provided the funding for this study under the code IR.IUMS.FMD.REC.1400.101. This

funding source had no role in the design of this study and will not have any role during its execution, analyses, interpretation of the data, or decision to submit results.

Funding

This work was supported by the [Iran University of Medical Sciences](#) [Grant number 19540].

CRedit authorship contribution statement

All authors have contributed significantly to the work. The author(s) declared no potential conflicts of interest with respect to the research, authorship, and/or publication of this article.

AHD: Writing – original draft, Methodology, Software, Conceptualization, Investigation, Data curation, Formal analysis, Visualization, Writing – review & editing.

AZS: Methodology, Software, Conceptualization, Investigation, Supervision, Resources, Funding acquisition, Writing – review & editing.

SKK: Investigation, Writing – review & editing.

Data availability statement

The data that support the findings of this study are available from the corresponding author upon reasonable request.

Human and animal rights

The authors declare that the work described has been carried out in accordance with the Declaration of Helsinki of the World Medical Association revised in 2013 for experiments involving humans as well as in accordance with the EU Directive 2010/63/EU for animal experiments.

Declaration of competing interest

The authors declare that they have no known competing financial interests or personal relationships that could have appeared to influence the work reported in this paper.

Acknowledgment

We thank the National Brain Mapping Laboratory for their support in MRI data acquisition and the Department of Medical Physics at Iran University of Medical Sciences for their assistance with the olfactory testing procedures.

References

- Acevedo M, Krueger JL. Two egocentric sources of the decision to vote: the voter's illusion and the belief in personal relevance. *Polit Psychol*. 2004;25(1):115–134.
- Bruine de Bruin W, Parker AM, Fischhoff B. Individual differences in adult decision-making competence. *J Pers Soc Psychol*. 2007;92(5):938–956. <https://doi.org/10.1037/0022-3514.92.5.938>.
- Dietrich C. Decision making: factors that influence decision making, heuristics used, and decision outcomes. *Inq J*. 2010;2(02).
- Stanovich KE, West RF. On the relative independence of thinking biases and cognitive ability. *J Pers Soc Psychol*. 2008;94(4):672–695. <https://doi.org/10.1037/0022-3514.94.4.672>.
- Vives ML, Heffner J, FeldmanHall O. Conceptual representations of uncertainty predict risky decision-making. *Cogn Affect Behav Neurosci*. 2023;23(3):491–502. <https://doi.org/10.3758/s13415-023-01090-8>.
- Jacobson PT, Vilarello BJ, Tervo JP, Waring NA, Gudis DA, Goldberg TE, Devanand DP, Overdeest JB. Associations between olfactory dysfunction and cognition: a scoping review. *J Neurol*. 2024;271(3):1170–1203. <https://doi.org/10.1007/s00415-023-12057-7>.
- Johnson AJ. Cognitive facilitation following intentional odor exposure. *Sens (Basel)*. 2011;11(5):5469–5488. <https://doi.org/10.3390/s110505469>.
- Lorig TS. Cognitive and non-cognitive effects of odour exposure: electrophysiological and behavioral evidence. *Psychol Biol Perfume*. 1992:161–173.
- Lyons SH, Gottfried JA. Predictive coding in the human olfactory system. *Trends Cogn Sci*. 2025;29(9):814–826. <https://doi.org/10.1016/j.tics.2025.04.005>.
- Moss M, Cook J, Wesnes K, Duckett P. Aromas of rosemary and lavender essential oils differentially affect cognition and mood in healthy adults. *Int J Neurosci*. 2003;113(1):15–38. <https://doi.org/10.1080/00207450390161903>.
- Moss M, Hewitt S, Moss L, Wesnes K. Modulation of cognitive performance and mood by aromas of peppermint and ylang-ylang. *Int J Neurosci*. 2008;118(1):59–77. <https://doi.org/10.1080/00207450601042094>.
- Moss M, Howarth R, Wilkinson L, Wesnes K. Expectancy and the aroma of Roman chamomile influence mood and cognition in healthy volunteers. *Int J Aromather*. 2006;16(2):63–73.
- Norrish MI, Dwyer KL. Preliminary investigation of the effect of peppermint oil on an objective measure of daytime sleepiness. *Int J Psychophysiol*. 2005;55(3):291–298. <https://doi.org/10.1016/j.ijpsycho.2004.08.004>.
- Warm JS, Dember WN, Parasuraman R. Effects of olfactory stimulation on performance and stress. *J Soc Cosmet Chem*. 1991;42(3):199–210.
- Gould A, Martin GN. A good odour to breathe? The effect of pleasant ambient odour on human visual vigilance. *Appl Cogn Psychol: Off J Soc Appl Res Mem Cogn*. 2001;15(2):225–232.
- Marchand S, Arsenault P. Odors modulate pain perception: a gender-specific effect. *Physiol Behav*. 2002;76(2):251–256. [https://doi.org/10.1016/s0031-9384\(02\)00703-5](https://doi.org/10.1016/s0031-9384(02)00703-5).
- Mitchell DJ, Kahn BE, Knasko SC. There's something in the air: effects of congruent or incongruent ambient odor on consumer decision making. *J Consum Res*. 1995;22(2):229–238.
- Roberts SC, Little AC, Lyndon A, Roberts J, Havlicek J, Wright RL. Manipulation of body odour alters men's self-confidence and judgements of their visual attractiveness by women. *Int J Cosmet Sci*. 2009;31(1):47–54.
- Villemure C, Slotnick BM, Bushnell MC. Effects of odors on pain perception: deciphering the roles of emotion and attention. *Pairing*. 2003;106(1–2):101–108.
- Ditto PH, Pizarro DA, Epstein EB, Jacobson JA, MacDonald TK. Visceral influences on risk-taking behavior. *J Behav Decis Mak*. 2006;19(2):99–113.
- Kechagia V, Drichoutis AC. The effect of olfactory sensory cues on willingness to pay and choice under risk. *J Behav Exp econ*. 2017;70:33–46.
- von Helversen B, Coppin G, Scheibehenne B. Money does not stink: using unpleasant odors as stimulus material changes risky decision making [journal article]. *J Behav Decis Mak*. 2020;33(5):593–605. <https://doi.org/10.1002/bdm.2178>.
- Gagarina A, Pikturienė I. The effect of ambient scent type and intensiveness on decision making heuristics. *Procedia - Soc Behav Sci*. 2015;213:605–609. <https://doi.org/10.1016/j.sbspro.2015.11.457>.
- Hirsch AR. Effects of ambient odors on slot-machine usage in a Las Vegas casino. *Psychol Mark*. 1995;12(7):585–594.
- Amina S. Uncus. In: Aminoff MJ, Daroff RB, eds. *Encyclopedia of the neurological sciences (Second edition)*. Academic Press; 2014:582–583. <https://doi.org/10.1016/B978-0-12-385157-4.01182-9>.
- Gottfried JA. Central mechanisms of odour object perception. *Nat Rev Neurosci*. 2010;11(9):628–641. <https://doi.org/10.1038/nrn2883>.
- Moini J, Piran P. Chapter 15 - limbic, olfactory, and gustatory systems. In: Moini J, Piran P, eds. *Functional and clinical neuroanatomy*. Academic Press; 2020:467–495. <https://doi.org/10.1016/B978-0-12-817424-1.00015-X>.
- Webb WG. 2 - Organization of the nervous system I. In: Webb WG, ed. *Neurology for the speech-language pathologist (Sixth edition)*. Mosby; 2017:13–43. <https://doi.org/10.1016/B978-0-323-10027-4.00002-6>.
- Royet JP, Plailly J, Delon-Martin C, Kareken DA, Segebarth C. fMRI of emotional responses to odors: influence of hedonic valence and judgment, handedness, and gender [Article]. *NeuroImage*. 2003;20(2):713–728. [https://doi.org/10.1016/S1053-8119\(03\)00388-4](https://doi.org/10.1016/S1053-8119(03)00388-4).
- de Wijk RA, Smeets PA, Polet IA, Holthuysen NT, Zoon J, Vingerhoeds MH. Aroma effects on food choice task behavior and brain responses to bakery food product cues. *Food Qual Prefer*. 2018;68:304–314.
- Homan P, Ely BA, Yuan M, Brosch T, Ng J, Trope Y, Schiller D. Aversive smell associations shape social judgment [Article]. *Neurobiol Learn Mem*. 2017;144:86–95. <https://doi.org/10.1016/j.nlm.2017.07.004>.
- Rolls ET, Grabenhorst F, Parris BA. Neural systems underlying decisions about affective odors. *J Cogn Neurosci*. 2010;22(5):1069–1082. <https://doi.org/10.1162/jocn.2009.21231>.
- Mallio CA, Buoso A, Stiffi M, Cea L, Vertulli D, Bernetti C, Di Gennaro G, van den Heuvel MP, Beomonte Zobel B. Mapping the neural basis of neuroeconomics with Functional Magnetic resonance imaging: a narrative literature review. *Brain Sci*. 2024;14(5). <https://doi.org/10.3390/brainsci14050511>.
- Li MT, Sun JW, Zhan LL, Antwi CO, Lv YT, Jia XZ, Ren J. The effect of seed location on functional connectivity: evidence from an image-based meta-analysis. *Front Neurosci*. 2023;17:1120741. <https://doi.org/10.3389/fnins.2023.1120741>.
- Knutson B, Adams CM, Fong GW, Hommer D. Anticipation of increasing monetary reward selectively recruits nucleus accumbens. *J Neurosci*. 2001;21(16):RC159. <https://doi.org/10.1523/JNEUROSCI.21-16-j0002.2001>.
- Oldham S, Murawski C, Fornito A, Youssef G, Yucel M, Lorenzetti V. The anticipation and outcome phases of reward and loss processing: a neuroimaging meta-analysis of the monetary incentive delay task. *Hum Brain Mapp*. 2018;39(8):3398–3418. <https://doi.org/10.1002/hbm.24184>.
- Kahneman D, Tversky A. Prospect theory: an analysis of decision under risk. *Handbook of the fundamentals of financial decision making: Part I*. World Scientific; 2013:99–127.
- Kuhnen CM, Knutson B. The neural basis of financial risk taking. *Neuron*. 2005;47(5):763–770. <https://doi.org/10.1016/j.neuron.2005.08.008>.

39. Rangel A, Camerer C, Montague PR. A framework for studying the neurobiology of value-based decision making. *Nat Rev Neurosci*. 2008;9(7):545–556. <https://doi.org/10.1038/nrn2357>.
40. Frasnelli J, Lundstrom JN, Schopf V, Negoias S, Hummel T, Lepore F. Dual processing streams in chemosensory perception. *Front Hum Neurosci*. 2012;6:288. <https://doi.org/10.3389/fnhum.2012.00288>.
41. Hummel T, Sekinger B, Wolf SR, Pauli E, Kobal G. Sniffin'sticks[®]: olfactory performance assessed by the combined testing of odor identification, odor discrimination and olfactory threshold. *Chem Senses*. 1997;22(1):39–52.
42. Kobal G, Hummel T, Sekinger B, Barz S, Roscher S, Wolf S. Sniffin'sticks[®]: screening of olfactory performance. *Rhinology*. 1996;34(4):222–226.
43. Kobal G, Klimek L, Wolfensberger M, Gudziol H, Temmel A, Owen C, Seeber H, Pauli E, Hummel T. Multicenter investigation of 1036 subjects using a standardized method for the assessment of olfactory function combining tests of odor identification, odor discrimination, and olfactory thresholds. *Eur Arch Oto-Rhino-Laryngol*. 2000;257(4):205–211.
44. Nieto-Castanon A. *Handbook of functional connectivity magnetic resonance imaging methods in CONN*. Hilbert Press; 2020.
45. Behzadi Y, Restom K, Liu J, Liu TT. A component based noise correction method (CompCor) for BOLD and perfusion based fMRI. *NeuroImage*. 2007;37(1):90–101. <https://doi.org/10.1016/j.neuroimage.2007.04.042>.
46. Fox MD, Snyder AZ, Vincent JL, Corbetta M, Van Essen DC, Raichle ME. The human brain is intrinsically organized into dynamic, anticorrelated functional networks. *Proc Natl Acad Sci*. 2005;102(27):9673–9678.
47. Fan L, Li H, Zhuo J, Zhang Y, Wang J, Chen L, Yang Z, Chu C, Xie S, Laird AR, Fox PT, Eickhoff SB, Yu C, Jiang T. The Human Brainnetome Atlas: a new brain atlas based on connectural architecture. *Cereb Cortex*. 2016;26(8):3508–3526. <https://doi.org/10.1093/cercor/bhw157>.
48. Brodmann K. Contributions to the histological localisation of the cerebral cortex VI announcement the arrangement of the cortex in humans. *J Psychol Neurol*. 1908;10:229–244.
49. Jung J, Lambon Ralph MA, Jackson RL. Subregions of DLPFC display graded yet distinct structural and functional connectivity. *J Neurosci*. 2022;42(15):3241–3252. <https://doi.org/10.1523/jneurosci.1216-21.2022>.
50. Petrides M, Pandya DN. Dorsolateral prefrontal cortex: comparative cytoarchitectonic analysis in the human and the macaque brain and corticocortical connection patterns. *Eur J Neurosci*. 1999;11(3):1011–1036. <https://doi.org/10.1460/9568.1999.00518.x>.
51. Walker AE. A cytoarchitectural study of the prefrontal area of the macaque monkey. *J Comp Neurol*. 1940;73(1):59–86.
52. Tzourio-Mazoyer N, Landeau B, Papathanassiou D, Crivello F, Etard O, Delcroix N, Mazoyer B, Joliot M. Automated anatomical labeling of activations in SPM using a macroscopic anatomical parcellation of the MNI MRI single-subject brain. *NeuroImage*. 2002;15(1):273–289. <https://doi.org/10.1006/nimg.2001.0978>.
53. Ito A, Yoshida K, Takeda K, Sawamura D, Murakami Y, Hasegawa A, Sakai S, Izuma K. The role of the ventromedial prefrontal cortex in automatic formation of impression and reflected impression. *Hum Brain Mapp*. 2020;41(11):3045–3058. <https://doi.org/10.1002/hbm.24996>.
54. Yoon L, Somerville LH, Kim H. Development of MPFC function mediates shifts in self-protective behavior provoked by social feedback. *Nat Commun*. 2018;9(1):3086. <https://doi.org/10.1038/s41467-018-05553-2>.
55. Chen B, Yang M, Liu M, Wang Q, Zhou H, Zhang M, Hou L, Wu Z, Zhang S, Lin G, Zhong X, Ning Y. Differences in olfactory functional connectivity in early-onset depression and late-onset depression. *Psychoradiology*. 2023;3. <https://doi.org/10.1093/psyrad/kkad030>.
56. Peter MG, Fransson P, Mårtensson G, Postma EM, Nordin LE, Westman E, Boesveldt S, Lundström JN. Normal olfactory functional connectivity despite lifelong absence of olfactory experiences. *Cereb Cortex*. 2021;31(1):159–168. <https://doi.org/10.1093/cercor/bhaa217>.
57. Seubert J, Freiherr J, Djordjevic J, Lundström JN. Statistical localization of human olfactory cortex. *NeuroImage*. 2013;66:333–342. <https://doi.org/10.1016/j.neuroimage.2012.10.030>.
58. Gottfried JA, O'Doherty J, Dolan RJ. Appetitive and aversive olfactory learning in humans studied using event-related functional magnetic resonance imaging. *J Neurosci*. 2002;22(24):10829–10837. <https://doi.org/10.1523/jneurosci.22-24-10829.2002>.
59. Oka N, Iwai K, Sakai H. The neural substrates responsible for food odor processing: an activation likelihood estimation meta-analysis. *Front Neurosci*. 2023;17:1191617. <https://doi.org/10.3389/fnins.2023.1191617>.
60. Zald DH, Pardo JV. Functional neuroimaging of the olfactory system in humans. *Int J Psychophysiol*. 2000;36(2):165–181. [https://doi.org/10.1016/s0167-8760\(99\)00110-5](https://doi.org/10.1016/s0167-8760(99)00110-5).
61. Eslinger PJ, Damasio AR. Severe disturbance of higher cognition after bilateral frontal lobe ablation: patient EVR. *Neurology*. 1985;35(12):1731–1741. <https://doi.org/10.1212/wnl.35.12.1731>.
62. Henri-Bhargava A, Simioni A, Fellows LK. Ventromedial frontal lobe damage disrupts the accuracy, but not the speed, of value-based preference judgments. *Neuropsychologia*. 2012;50(7):1536–1542. <https://doi.org/10.1016/j.neuropsychologia.2012.03.006>.
63. Koenigs M, Tranel D. Irrational economic decision-making after ventromedial prefrontal damage: evidence from the Ultimatum Game. *J Neurosci*. 2007;27(4):951–956. <https://doi.org/10.1523/JNEUROSCI.4606-06.2007>.
64. Pujara MS, Wolf RC, Baskaya MK, Koenigs M. Ventromedial prefrontal cortex damage alters relative risk tolerance for prospective gains and losses. *Neuropsychologia*. 2015;79(Pt A):70–75. <https://doi.org/10.1016/j.neuropsychologia.2015.10.026>.
65. Tashjian SM, Cussen J, Deng W, Zhang B, Mobbs D. Subregions in the ventromedial prefrontal cortex integrate threat and protective information to meta-represent safety. *PLoS Biol*. 2025;23(1):e3002986. <https://doi.org/10.1371/journal.pbio.3002986>.
66. Arana FS, Parkinson JA, Hinton E, Holland AJ, Owen AM, Roberts AC. Dissociable contributions of the human amygdala and orbitofrontal cortex to incentive motivation and goal selection. *J Neurosci*. 2003;23(29):9632–9638. <https://doi.org/10.1523/JNEUROSCI.23-29-09632.2003>.
67. Cox SM, Andrade A, Johnsrude IS. Learning to like: a role for human orbitofrontal cortex in conditioned reward. *J Neurosci*. 2005;25(10):2733–2740. <https://doi.org/10.1523/JNEUROSCI.3360-04.2005>.
68. Elliott R, Agnew Z, Deakin JF. Hedonic and informational functions of the human orbitofrontal cortex. *Cereb Cortex*. 2010;20(1):198–204. <https://doi.org/10.1093/cercor/bhp092>.
69. FitzGerald TH, Seymour B, Dolan RJ. The role of human orbitofrontal cortex in value comparison for incommensurable objects. *J Neurosci*. 2009;29(26):8388–8395. <https://doi.org/10.1523/JNEUROSCI.0717-09.2009>.
70. Gottfried JA, O'Doherty J, Dolan RJ. Encoding predictive reward value in human amygdala and orbitofrontal cortex. *Science*. 2003;301(5636):1104–1107. <https://doi.org/10.1126/science.1087919>.
71. Hubbard EM, Piazza M, Pinel P, Dehaene S. Interactions between number and space in parietal cortex. *Nat Rev Neurosci*. 2005;6(6):435–448.
72. Kadosh RC, Henik A, Rubinsten O, Mohr H, Dori H, Van De Ven V, Zorzi M, Hendler T, Goebel R, Linden DE. Are numbers special?: the comparison systems of the human brain investigated by fMRI. *Neuropsychologia*. 2005;43(9):1238–1248.
73. Krawczyk DC. Contributions of the prefrontal cortex to the neural basis of human decision making. *Neurosci Biobehav Rev*. 2002;26(6):631–664. [https://doi.org/10.1016/s0149-7634\(02\)00021-0](https://doi.org/10.1016/s0149-7634(02)00021-0).
74. Kringelbach ML, O'Doherty J, Rolls ET, Andrews C. Activation of the human orbitofrontal cortex to a liquid food stimulus is correlated with its subjective pleasantness. *Cereb Cortex*. 2003;13(10):1064–1071.
75. Kringelbach ML, Rolls ET. The functional neuroanatomy of the human orbitofrontal cortex: evidence from neuroimaging and neuropsychology. *Prog Neurobiol*. 2004;72(5):341–372. <https://doi.org/10.1016/j.neurobio.2004.03.006>.
76. O'Doherty J, Kringelbach ML, Rolls ET, Hornak J, Andrews C. Abstract reward and punishment representations in the human orbitofrontal cortex. *Nat Neurosci*. 2001;4(1):95–102. <https://doi.org/10.1038/82959>.
77. Plassmann H, O'Doherty J, Rangel A. Orbitofrontal cortex encodes willingness to pay in everyday economic transactions. *J Neurosci*. 2007;27(37):9984–9988. <https://doi.org/10.1523/JNEUROSCI.2131-07.2007>.
78. Sugrue LP, Corrado GS, Newsome WT. Choosing the greater of two goods: neural currencies for valuation and decision making. *Nat Rev Neurosci*. 2005;6(5):363–375. <https://doi.org/10.1038/nrn1666>.
79. Wang BA, Veissmann M, Banerjee A, Pleger B. Human orbitofrontal cortex signals decision outcomes to sensory cortex during behavioral adaptations. *Nat Commun*. 2023;14(1):3552. <https://doi.org/10.1038/s41467-023-38671-7>.
80. Brewer JA, Worhunsky PD, Carroll KM, Rounsaville BJ, Potenza MN. Pretreatment brain activation during stroop task is associated with outcomes in cocaine-dependent patients. *Biol Psychiatry*. 2008;64(11):998–1004.
81. Egan MF, Goldberg TE, Kolachana BS, Callicott JH, Mattay CS, Straub RE, Goldman D, Weinberger DR. Effect of COMT Val108/158 met genotype on frontal lobe function and risk for schizophrenia. *Proc Natl Acad Sci U S A*. 2001;98(12):6917–6922. <https://doi.org/10.1073/pnas.111134598>.
82. Hanlon CA, Dowdle LT, Jones JL. Biomarkers for success: using neuroimaging to predict relapse and develop brain stimulation treatments for cocaine-dependent individuals. *Int Rev Neurobiol*. 2016;129:125–156. <https://doi.org/10.1016/bs.irn.2016.06.006>.
83. Lin C, Wang Y, Xia W, Zhang D, Wang X, Wang Y, Du Y, Yu H, Ji S. Neural mechanisms of maladaptive risk decision-making across psychiatric disorders. *Front Behav Neurosci*. 2025;19:1637582. <https://doi.org/10.3389/fnbeh.2025.1637582>.
84. Pereira DJ, Pereira J, Sayal A, Morais S, Macedo A, Direito B, Castelo-Branco M. Functional and structural connectivity success predictors of real-time fMRI neuro-feedback targeting DLPFC: contributions from central executive, salience, and default mode networks. *Netw Neurosci*. 2024;8(1):81–95. https://doi.org/10.1162/netn_a_00338.
85. Fermin ASR, Friston K, Yamawaki S. An insula hierarchical network architecture for active interoceptive inference. *R Soc Open Sci*. 2022;9(6):220226. <https://doi.org/10.1098/rsos.220226>.
86. Bechara A, Damasio AR. The somatic marker hypothesis: a neural theory of economic decision. *Games Econ Behav*. 2005;52(2):336–372.
87. Menon V, Uddin LQ. Saliency, switching, attention and control: a network model of insula function. *Brain Struct Funct*. 2010;214(5–6):655–667. <https://doi.org/10.1007/s00429-010-0262-0>.
88. Naqvi NH, Bechara A. The hidden island of addiction: the insula. *Trends Neurosci*. 2009;32(1):56–67. <https://doi.org/10.1016/j.tins.2008.09.009>.
89. Tops M, Boksem MA. A potential role of the inferior frontal gyrus and anterior insula in cognitive control, brain rhythms, and event-related potentials. *Front Psychol*. 2011;2:330. <https://doi.org/10.3389/fpsyg.2011.00330>.
90. Venkatraman V, Payne JW, Bettman JR, Luce MF, Huettel SA. Separate neural mechanisms underlie choices and strategic preferences in risky decision making. *Neuron*. 2009;62(4):593–602. <https://doi.org/10.1016/j.neuron.2009.04.007>.
91. Zhang R, Deng H, Xiao X. The insular cortex: an interface between sensation, emotion and cognition. *Neurosci Bull*. 2024;40(11):1763–1773. <https://doi.org/10.1007/s12264-024-01211-4>.
92. Xue G, Lu Z, Levin IP, Bechara A. The impact of prior risk experiences on subsequent risky decision-making: the role of the insula. *NeuroImage*. 2010;50(2):709–716. <https://doi.org/10.1016/j.neuroimage.2009.12.097>.

93. Howard JD, Plailly J, Grueschow M, Haynes JD, Gottfried JA. Odor quality coding and categorization in human posterior piriform cortex. *Nat Neurosci.* 2009;12(7):932–938. <https://doi.org/10.1038/nn.2324>.
94. Erzurumlu R, Sengul G, Ulupinar E. Chapter 7 - limbic system. In: Erzurumlu R, Sengul G, Ulupinar E, eds. *Human neuroanatomy*. Academic Press; 2024:95–119. <https://doi.org/10.1016/B978-0-323-99725-6.00007-9>.
95. Bao X, Raguette LL, Cole SM, Howard JD, Gottfried J. The role of piriform associative connections in odor categorization. *Elife.* 2016;5. <https://doi.org/10.7554/eLife.13732>.
96. Burgess PW, Dumoutheil I, Gilbert SJ. The gateway hypothesis of rostral prefrontal cortex (area 10) function. *Trends Cogn Sci.* 2007;11(7):290–298. <https://doi.org/10.1016/j.tics.2007.05.004>.
97. Fishbein DH, Eldredh DL, Hyde C, Matochik JA, London ED, Contoreggi C, Kurian V, Kimes AS, Breeden A, Grant S. Risky decision making and the anterior cingulate cortex in abstinent drug abusers and nonusers. *Brain Res Cogn Brain Res.* 2005;23(1):119–136. <https://doi.org/10.1016/j.cogbrainres.2004.12.010>.
98. Grabenhorst F, Rolls ET, Parris BA. From affective value to decision-making in the prefrontal cortex. *Eur J Neurosci.* 2008;28(9):1930–1939. <https://doi.org/10.1111/j.1460-9568.2008.06489.x>.
99. Kim JN, Shadlen MN. Neural correlates of a decision in the dorsolateral prefrontal cortex of the macaque. *Nat Neurosci.* 1999;2(2):176–185. <https://doi.org/10.1038/5739>.
100. Morris G, Nevet A, Arkadir D, Vaadia E, Bergman H. Midbrain dopamine neurons encode decisions for future action. *Nat Neurosci.* 2006;9(8):1057–1063. <https://doi.org/10.1038/nn1743>.
101. Rushworth MF, Behrens TE, Rudebeck PH, Walton ME. Contrasting roles for cingulate and orbitofrontal cortex in decisions and social behaviour. *Trends Cogn Sci.* 2007;11(4):168–176. <https://doi.org/10.1016/j.tics.2007.01.004>.
102. Thielscher A, Pessoa L. Neural correlates of perceptual choice and decision making during fear–disgust discrimination. *J Neurosci.* 2007;27(11):2908–2917.
103. Greene JD, Nystrom LE, Engell AD, Darley JM, Cohen JD. The neural bases of cognitive conflict and control in moral judgment. *Neuron.* 2004;44(2):389–400. <https://doi.org/10.1016/j.neuron.2004.09.027>.
104. Hearne LJ, Cocchi L, Zalesky A, Mattingley JB. Reconfiguration of brain network architectures between resting-state and complexity-dependent cognitive reasoning. *J Neurosci.* 2017;37(35):8399–8411.
105. Morin TM, Moore KN, Isenburg K, Ma W, Stern CE. Functional reconfiguration of task-active frontoparietal control network facilitates abstract reasoning. *Cereb Cortex.* 2023;33(10):5761–5773. <https://doi.org/10.1093/cercor/bhac457>.
106. Hampton AN, Adolphs R, Tysza MJ, O'Doherty JP. Contributions of the amygdala to reward expectancy and choice signals in human prefrontal cortex. *Neuron.* 2007;55(4):545–555. <https://doi.org/10.1016/j.neuron.2007.07.022>.
107. Heekeren HR, Marrett S, Bandettini PA, Ungerleider LG. A general mechanism for perceptual decision-making in the human brain. *Nature.* 2004;431(7010):859–862. <https://doi.org/10.1038/nature02966>.
108. Knutson B, Rick S, Wimmer GE, Prelec D, Loewenstein G. Neural predictors of purchases. *Neuron.* 2007;53(1):147–156. <https://doi.org/10.1016/j.neuron.2006.11.010>.
109. Lamichhane B, Adhikari BM, Dhamala M. The activity in the anterior insulae is modulated by perceptual decision-making difficulty. *Neuroscience.* 2016;327:79–94. <https://doi.org/10.1016/j.neuroscience.2016.04.016>.
110. Liu X, Hairston J, Schrier M, Fan J. Common and distinct networks underlying reward valence and processing stages: a meta-analysis of functional neuroimaging studies. *Neurosci Biobehav Rev.* 2011;35(5):1219–1236. <https://doi.org/10.1016/j.neubiorev.2010.12.012>.
111. Mohr PN, Biele G, Krugel LK, Li SC, Heekeren HR. Neural foundations of risk-return trade-off in investment decisions. *NeuroImage.* 2010;49(3):2556–2563. <https://doi.org/10.1016/j.neuroimage.2009.10.060>.
112. Bach DR, Seymour B, Dolan RJ. Neural activity associated with the passive prediction of ambiguity and risk for aversive events. *J Neurosci.* 2009;29(6):1648–1656. <https://doi.org/10.1523/JNEUROSCI.4578-08.2009>.
113. Fujino J, Hirose K, Tei S, Kawada R, Tsurumi K, Matsukawa N, Miyata J, Sugihara G, Yoshihara Y, Ideno T, Aso T, Takemura K, Fukuyama H, Murai T, Takahashi H. Ambiguity aversion in schizophrenia: an fMRI study of decision-making under risk and ambiguity. *Schizophr Res.* 2016;178(1–3):94–101. <https://doi.org/10.1016/j.schres.2016.09.006>.
114. Huettel SA. Behavioral, but not reward, risk modulates activation of prefrontal, parietal, and insular cortices. *Cogn Affect Behav Neurosci.* 2006;6(2):141–151. <https://doi.org/10.3758/cabn.6.2.141>.
115. Krain AL, Wilson AM, Arbuckle R, Castellanos FX, Milham MP. Distinct neural mechanisms of risk and ambiguity: a meta-analysis of decision-making. *NeuroImage.* 2006;32(1):477–484. <https://doi.org/10.1016/j.neuroimage.2006.02.047>.
116. Levy I, Snell J, Nelson AJ, Rustichini A, Glimcher PW. Neural representation of subjective value under risk and ambiguity. *J Neurophysiol.* 2010;103(2):1036–1047. <https://doi.org/10.1152/jn.00853.2009>.
117. Hampton AN, O'Doherty J. Decoding the neural substrates of reward-related decision making with functional MRI. *Proc Natl Acad Sci U S A.* 2007;104(4):1377–1382. <https://doi.org/10.1073/pnas.0606297104>.